

# Simulation Standard

TCAD Driven CAD

A Journal for Process and Device Engineers

## Yield Analysis and Performance Optimization Using *FastBlaze* and *SPAYN*

### Introduction

In previous *Simulation Standard* articles (Nov 97 & Nov 98) *FastBlaze* has been presented as a new, highly efficient approach to simulating advanced HEMTs and MESFETs.

Conventional device simulators often suffer from slow execution times, leading to a trade off between mesh density and physical model complexity against CPU run time and convergence. This requires engineers to compromise accuracy to achieve a reasonable throughput.

By focusing solely upon FET simulation, *FastBlaze* has been able to greatly optimize the physical solution procedure, enabling the use of the most sophisticated physical models while maintaining a fast execution (typically less than 1 minute for a full set of DC  $I_D$ - $V_{DS}$  curves) This speed enables both complex and extensive experimental designs to be completed on a reasonable time scale, permitting experiments that would be prohibitively expensive for more traditional device simulators.

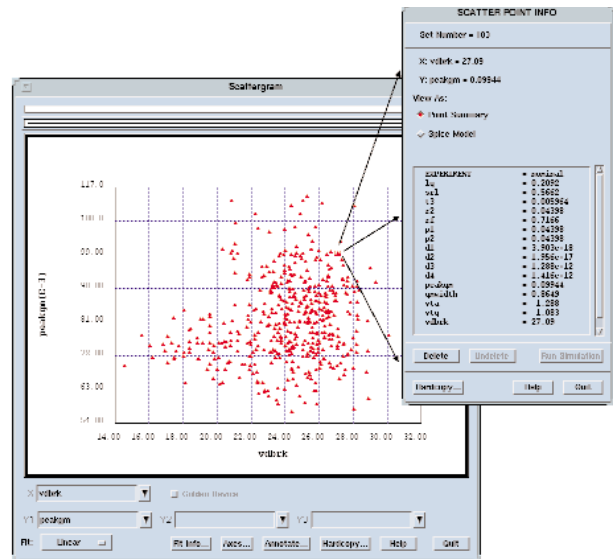


Figure 1. Scatter plot showing  $V_{Dbrk}$  vs.  $gm_{pk}$  from Monte Carlo experiment.

### Experimental Design

In this exercise we illustrate the power of *FastBlaze*, when coupled to *SPAYN* by implementing a simple but large experimental design.

We took a relatively complicated double-recessed, double delta-doped pHEMT structure (Figure 2.) and randomly varied 9 of the physical input parameters (see Table 1).

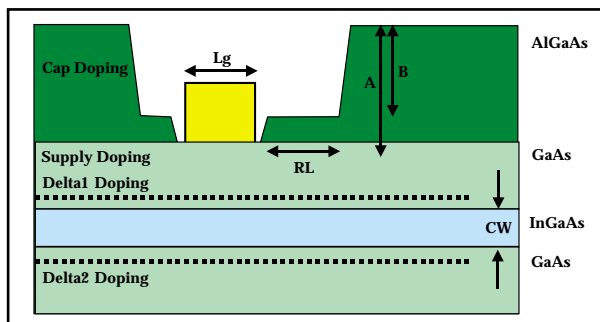


Figure 2. Double recessed, double  $\delta$ -doped pHEMT structure.

There are two common distribution choices for Monte Carlo experimental design, a uniform random distribution suits device optimization, as the input parameter plane is more efficiently covered, however, by using a Gaussian profile, which is more representative of natural variations in the device, we can also perform yield analysis directly upon the experimental output.

Continued on page 2....

INSIDE	
New Model for Simulation of Exposure Process in Complex Nonplanar resist-Substrate Structures . . . . .	4
Fast, Physical, Predictive and Calibrated Modeling of Ion Implantation . . . . .	5
Calendar of Events . . . . .	10
Hints, Tips, and Solutions . . . . .	11

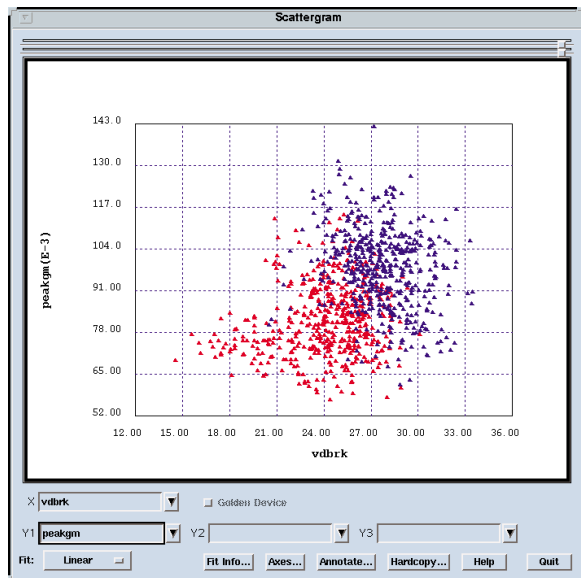


Figure 3. Scatter plot showing  $V_{Dbrk}$  vs.  $gm_{pk}$  for both the nominal and optimized device structures.

## Device Optimization

When the results from the Monte Carlo experiment are investigated in *SPAYN* the user can identify "good" devices by visually inspecting the scatter plots. In Figure 1 a device has been chosen with both high  $gm_{pk}$  and breakdown. *SPAYN* then displays each of the input variables for that simulation in a pop-up box.

A simple yet effective method of optimization is then to center the input values on this "good" device and re-run the whole experiment. Figure 3 displays the combined scatter plots for both experiments, showing a marked improvement in both  $gm_{pk}$  and  $V_{Dbrk}$ .

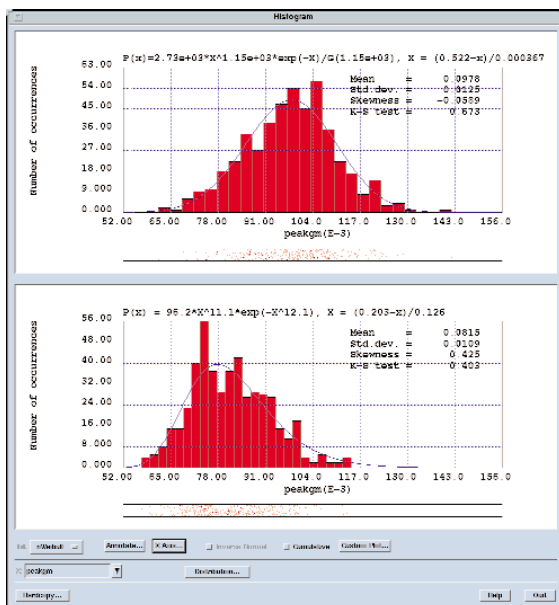


Figure 4. Distribution analysis. Here the mean value of both  $V_{Dbrk}$  and  $gm_{pk}$  have been increased in the optimized structure with no significant change in the standard deviations.

predictor (input) variables	
Lg	gate length
RL	second recess length
CW	InGas channel thickness
A	total recess depth
rf	recess fraction, B/A
d1	cap doping density
d2	supply doping density
d3	1st $\delta$ doping density
d4	2nd $\delta$ doping density
response (target) variables	
$gm_{pk}$	peak transconductance
$V_{Dbrk}$	break down voltage

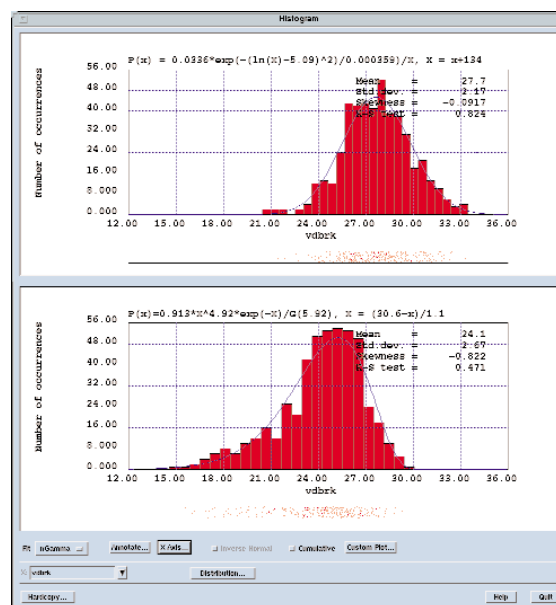
Table 1. Input and response variables for the experiment.

Figure 4 shows histograms of both  $gm_{pk}$  and  $V_{Dbrk}$  for the nominal and optimized cases. The qualitative improvement in the parameters is immediately observable, with the mean  $gm_{pk}$  increasing from 410 to 490 mS/mm and  $V_{Dbrk}$  from 24 to 28 V. Further there is no significant change in the standard deviation of either distribution.

## Yield Analysis

Since both experiments were performed using Gaussian distributions the output distribution functions can be evaluated directly to obtain the yield values.

In our example we choose an arbitrary "fail" point for the breakdown voltage and integrate both the nominal and optimized distributions to calculate the expected yield from a wafer. Choosing a minimum of 20 Volts



	Lg	RL	CW	A	rf	d1	d3	gm <sub>pk</sub>	V <sub>Dbrk</sub>
Lg	1.00	-0.30	0.49	0.46	0.11	0.35	0.47	-0.39	-0.50
RL	-0.30	1.00	-0.32	-0.32	-0.07	-0.24	-0.27	0.27	0.62
CW	0.49	-0.32	1.00	0.44	0.15	0.37	0.44	-0.32	-0.44
A	0.46	-0.32	0.44	1.00	0.09	0.34	0.40	-0.35	-0.58
rf	0.11	-0.07	0.15	0.09	1.00	0.08	0.11	-0.17	-0.27
d1	0.35	-0.24	0.37	0.34	0.08	1.00	0.30	-0.28	-0.40
d3	0.47	-0.27	0.44	0.40	0.11	0.30	1.00	-0.34	-0.41
gm <sub>pk</sub>	-0.39	0.27	-0.32	-0.35	-0.17	-0.28	-0.34	1.00	0.32
V <sub>Dbrk</sub>	-0.50	0.62	-0.44	-0.58	-0.27	-0.40	-0.41	0.32	1.00

Table 2. A bridged correlation matrix for the combined nominal and optimized experimental data.

breakdown the yield from the nominal structure is 92.2% where as the optimized is greater than 99%. If the minimum is shifted to 22 Volts, the nominal structure's yield drops to 80% where as the optimized is still greater than 98%.

### SPAYN Parameter Analysis

The previous examples demonstrate a straight forward optimization technique, however, the inter-dependencies of each input parameter have not been analyzed. *SPAYN* provides the tools for investigating these relationships via the correlation matrix.

*SPAYN* can also be used to generate an analytical "black box" model of this data set through regression analysis. This is more computationally efficient than *FastBlaze* however is strictly limited to this structure.

For more information on the techniques described below please refer to the *SPAYN User's Manual*.

### Correlation

*SPAYN* can be used to investigate the inter-parameter dependencies through the correlation matrix. An abridged matrix showing the most significant variables is presented in Table 2.

This is useful when determining which parameters will have a larger influence in the regression models. In this case we can see that the gate length, second recess length and the total recess depth are highly correlated with V<sub>Dbrk</sub> ( $|r| > 0.5$ ).

### Regression

Regression analysis can be performed within *SPAYN* to generate response surfaces for the target parameters. These regression equations can then be used to predict new values for the response variables far more efficiently than by using any physical simulator.

Using V<sub>Dbrk</sub> as the response variable and the 9 predictor parameters from Table 1, an analysis of variance (ANOVA) was performed to identify the most suitable

Source	DF	MS	Fcrit	P-val	Adj. R <sup>2</sup>
1. Linear model	9	613.4	274.7	v.sig.	.63
2. Extra due to interactions (xy) terms	36	21.6	9.7	v.sig.	.71
3. Extra due to quadratic (x <sup>2</sup> ) terms	9	18.6	8.4	v.sig.	.73
4. Extra due to interactions (xyz) terms	84	3.7	1.7	not sig.	.78
5. Extra due to interactions (xy <sup>2</sup> ) terms	72	2.8	1.3	not sig.	.76
6. Extra due to cubic (x <sup>3</sup> ) terms	9	4.5	2.0	not sig.	.75
Error (residual)	742	2.2			
Total	961				

Table 3. Analysis of variance (ANOVA) for V<sub>Dbrk</sub>.

model. If a more complete ANOVA analysis was required, an engineer might also add or remove individual parameters.

There are several model selection criterion available, the most commonly used being p-value and adjusted R<sup>2</sup>.

From the ANOVA table (table 3) all of the p-values up to model 3. are highly significant, hence our regression model should include all linear (x), interaction (xy) and quadratic terms (x<sup>2</sup>). Adding extra parameters to the regression equation (models 4,5 and 6) produce non-significant p-values, indicating that it is not worth including them in the model.

As an alternative we can also use the adjusted R<sup>2</sup> value as the selection criterion. In this case model 4 should be used i.e. all linear (x), interaction (xy), quadratic (x<sup>2</sup>) and interaction (xyz) terms.

*Continued on page 6...*

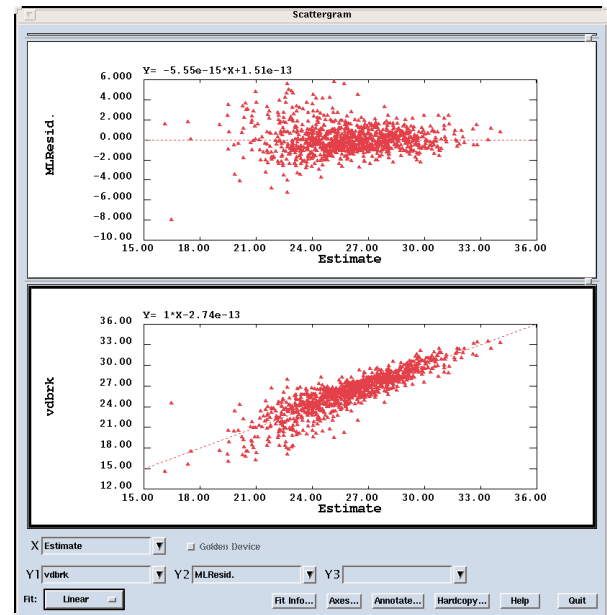


Figure 5. Residual analysis of model 4.

# New Model for Simulation of Exposure Process in Complex Nonplanar Resist-Substrate Structures

## 1. Introduction

Predictive and efficient lithography simulation is an important component of the semiconductor industry efforts to develop the next generation of deep submicron technologies. Emerging technologies are based on elements with very small feature sizes and extremely complex and nonplanar topographies. Therefore lithography processing has to provide high resolution with large depth of focus. Simultaneously such effects as nonplanar reflections and notching as well as refractive index dependence on local absorbed dose are very critical for printing small mask elements using short wavelength radiation. This work presents a new approach for simulating the exposure process, which takes into account these effects in complex nonplanar resist-substrate structures. The method is based on numerical solution of the Helmholtz equation for the electric field in the media with complex refractive index  $n(x,y,z,I)$ , where  $I$  is the dose previously absorbed at the point. Propagation of initial electromagnetic field and fields reflected from the material interface elements are calculated using the Beam Propagation Method (BPM) [1]. Because the method is very general it can be used for different types of radiation (UV, EUV, X-ray) as well as for multiexposure processes and multilayer and nonlinear resists. The method is implemented as a separate module, which is interfaced with imaging and developing modules of *Optolith*. Complete exposure simulations for a typical 2D structure take 2-20 sec on a Sun Ultra-10 workstation.

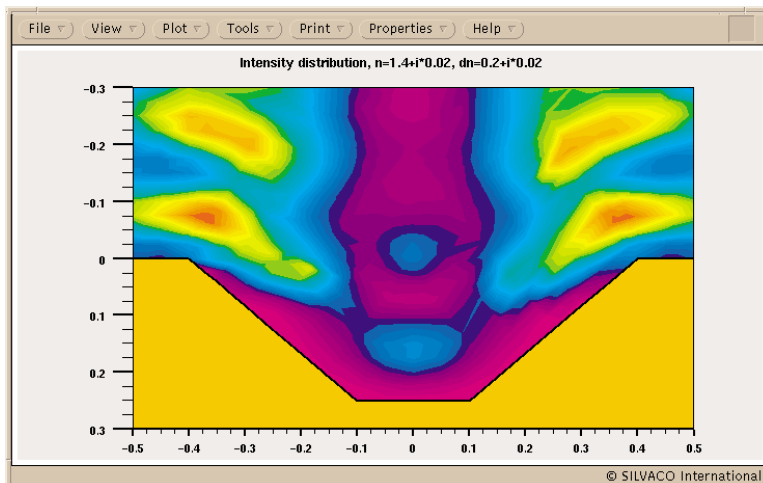


Figure 2. The distribution of intensity (dose) in the resist over a non-planar substrate. The resist refractive index is modified during the exposure from for unexposed resist to for completely exposed one.

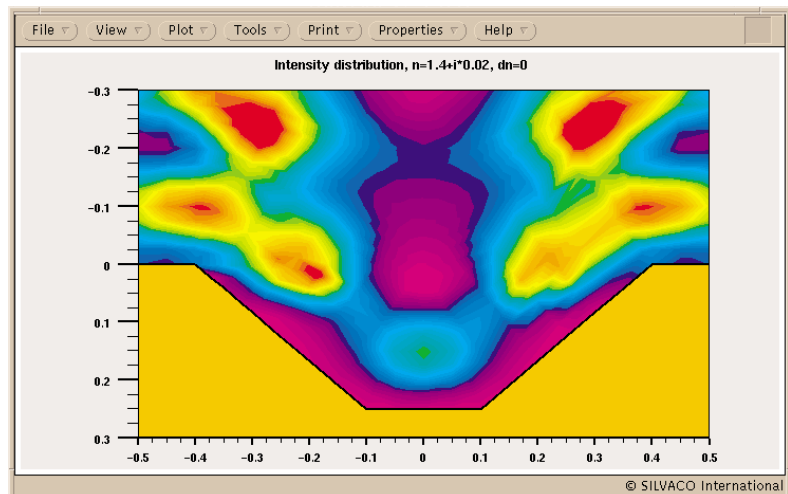


Figure 1. The distribution of intensity (dose) in the resist over a non-planar substrate. The resist refractive index is not modified during the exposure.

## 2. Model

The exposure model previously implemented into *Optolith* is based on the Ray Tracing Method (RTM). RTM cannot accurately calculate diffraction on small features and does not allow to account for optical nonlinearities of the photoresist. The new exposure model has been developed to achieve several goals:

1. More accurate simulation of the exposure process by taking into account diffraction effects.
2. Include a capability to simulate non-linear effect of the intensity distribution on the local optical properties of the resist material.
3. Improve the simulator performance.

The Beam Propagation Method (BPM) is used to solve the Helmholtz equation for electromagnetic field inside the structure. During the simulation the field distribution is formed as the superposition of incident light, all the reflections from all elements of the resist-substrate interface and secondary reflection(s) from the upper resist surface.

The formal descriptions of the BPM can be found in [1]. In [2-4] some applications using BPM are described too.

In this model the Helmholtz equation for the electric field  $E$  into the media with complex refractive index  $n(x, y, z)$

$$\nabla^2 E + k^2 n^2 E = 0$$

where  $k$  is the wave number, is solved in two main stages:

1. First, the diffraction over a small spatial step along the propagation is calculated thus obtaining the new field amplitude distribution without absorption taken into account;
2. Then the actual field distribution is computed as a product of this amplitude distribution and the distribution of the complex absorption over the step.

Let the wave is propagated along  $z$ -axis. We find the solution as a quasi plane wave  $E=A(x, y, z)\exp(inkz)$  with slowly varied amplitude  $A$  ( $A$  is modified with  $z$  slower than phase term  $inkz$ ). In this case, the Fourier image of current distribution  $A$  in the plane  $z=z_0$  is defined as

$$F_A(k_x, k_y) = \int A(x, y, z_0) \exp[-i(k_x x + k_y y)] dx dy.$$

After propagating over a small step each component of obtains additional phase shift corresponded to the value of  $k_z = \sqrt{k^2 - k_x^2 - k_y^2}$ . Thus, the amplitude distribution at  $z = z_0 + \Delta z$  (without accounting for absorption) can be written as

$$A(x, y, z_0 + \Delta z) = \int F_A(k_x, k_y) \exp(ik_z \Delta z) \exp[i(k_x x + k_y y)] dk_x dk_y.$$

Due to difference of actual optical properties from ones for vacuum, the field at the new plane  $z = z_0 + \Delta z$  is computed simply:

$$E(x, y, z_0 + \Delta z) = A(x, y, z_0 + \Delta z) \exp\{ik[n(x, y, z) - 1]\Delta z\}.$$

The algorithm is repeated recursively step-by-step over all simulation domain. The same calculations are applied to reflections from all segments of the resist boundaries. And the whole procedure is repeated NUM.REFL times, where NUM.REFL is specified in the EXPOSURE statement.

This approach allows the dependence of the refraction index  $n$  on intensity  $I$  to be taken into account. The following formula for  $n(x, y, z, I)$  is implemented:

$$n(x, y, z, I) = n_{\text{unexposed}} + (n_{\text{unexposed}} - n_{\text{exposed}}) [1 - M_{\text{PAC}}(x, y, z, I)].$$

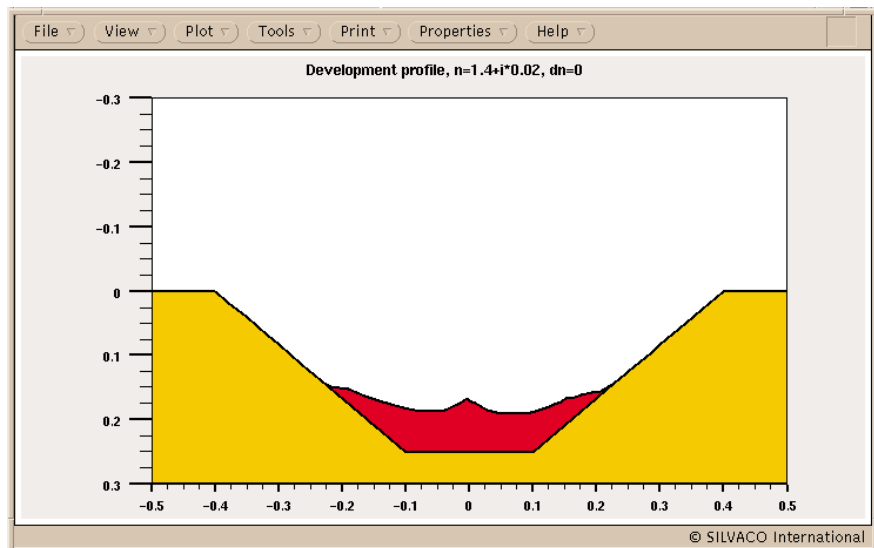


Figure 3. The resist development profile corresponding to the dose distribution in Figure 1.

Here  $\frac{\partial M_{\text{PAC}}}{\partial t} = -CI(x, y, z, t)M_{\text{PAC}}$ , where  $I(x, y, z, t)$  is the current intensity distribution,  $C$  is the Mack's C-parameter. This effect is calculated by accumulating the total dose in several steps so the intensity distribution is formed as the sum of distributions obtained for each step. In this case, the previously accumulated intensities are used to compute current values of the refractive index for each point inside the resist area.

### 3. Changes in Optolith Syntax

Several additional parameters have been included in the OPTOLITH syntax to control the new model. The BPM parameter in the EXPOSURE statement specifies that Beam Propagation Method is to be used during exposure simulation. This parameter is now default. If the RTM parameter is specified instead the old Ray Tracing Method will be used.

To simulate the dose effect on the resist optical properties the difference of the complex refraction index for exposed and unexposed resist has to be specified. It is assumed that standard value of the refraction index corresponds to the case of unexposed resist. The following OPTICAL statement:

```
optical name.resist=RESIST1 i.line
delta.real=0.1 delta.imag=-0.03
```

specifies that the real part of the refraction index increases by 0.1 for completely exposed resist while the imaginary part of the refraction index (absorption) is reduced by 0.03 for completely exposed resist.

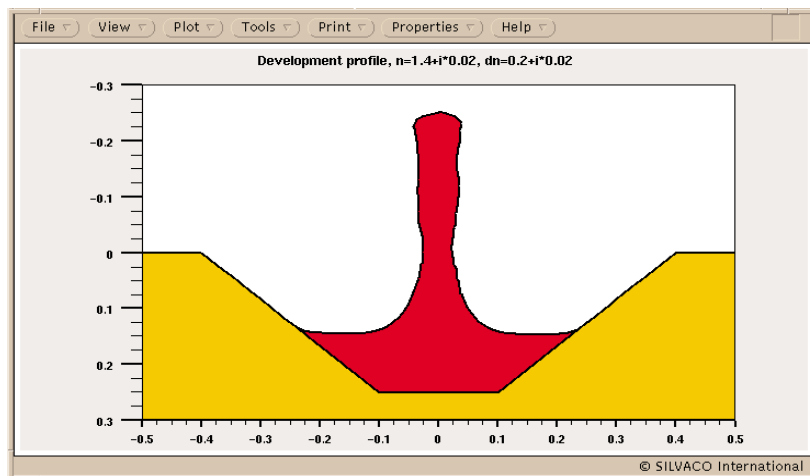


Figure 4. The resist development profile corresponding to the dose distribution in Figure 2.

#### 4. Example

The figures illustrate influence of the "dose effect" on the developed profile. Artificial conditions were simulated to outline the importance of the dose effect. In Figure 1 and 2 the intensity distributions in the resist over a non-planar substrate are shown for the cases of constant refraction index  $n_0 = 1.4 + i \cdot 0.02$  (Figure 1) and the index varied with dose from  $n_0$  for unexposed resist to  $n_1 = 1.4 + i \cdot 0.04$  for completely exposed one (Figure 2). The exposure level near the center of the substrate deepening differs substantially for these two cases. In the both cases there is the local maximum of the intensity due to reflections from the slope walls. However, in the

second case, this maximum is visibly lower due to modification of the resist properties during the exposure. These quantitative differences in the intensity distributions result in completely different resist development profiles (see Figure 3, 4). In the first case the feature is unresolved (Figure 3) while in the second case (Figure 4) the whole lithography process was successful.

New capabilities of the *Optolith* simulator allow to determine the characteristics of actual resists as well as to optimize parameters of the technological process.

#### References

- [1] J. Van Roey, J. van der Donk, P.E. Lagasse. Beam-propagation method: analysis and assessment. *J. Opt.Soc. Am.*, Vol.71, No. 7, July 1981, p. 803.
- [2] J. Z. Y. Guo, F. Cerrina. Modeling X-ray proximity lithography. *IBM J. Res. Develop.*, Vol. 37, No. 3, May 1993, p. 331.
- [3] A. Erdmann, C. L. Henderson, C. G. Wilson, W. Henke. Influence of optical nonlinearities of the photoresist on the photolithographic process: basics. *SPIE Proc.*, Vol. 3051, 1997, p. 529.
- [4] A. Erdmann, C. L. Henderson, C. G. Wilson, R. R. Dammel. Some aspects of thick film resist performance and modeling. *SPIE Proc.*, Vol. 3333, 1998, p. 1201.

...continued from page 3

The computational demands for evaluating a regression model are minimal when compared to a full physical simulation, hence we chose model 4 from the ANOVA table.

After fitting the regression equation a residual analysis is performed to check the model. This is accomplished by plotting the residuals against the estimated values and also individual predictor variables (see Figure 5)

A visual inspection of these plots should not reveal any discernible trends. If any patterns were apparent this would indicate a poor model and further analysis would be required.

Finally the response surface was then used in place of *FastBlaze* to re-generate the original Monte Carlo data. Note: 1000 samples were simulated in under 1 second on a Sun ULTRA 10 workstation.  $V_{Dbrk}$  was then compared between the two data sets, the first generated by *FastBlaze* and the second via the *SPAYN* regression model. A deviation of less than 5% was typically observed, illustrating the validity of this approach.

#### Conclusions

By looking at the input parameters from the simulated "good" devices we can draw some conclusions about general design criteria for this type of device. First we have obvious changes, decreasing the gate length and increasing the second recess length to increase gm and breakdown respectively. The recess fraction, the ratio of 1st and total recess depths should be fixed for this structure at 0.8. Finally, the doping density of the 1st delta should be lowered to increase breakdown, whilst raising the density of the 2nd delta to maintain gm.

The *SPAYN* statistical analysis was used to confirm the device optimization and corresponding improvement in yield. Further, the correlation matrix revealed which input parameters are most significant.

An analysis of variance was performed to select an appropriate regression model which was checked with a residual analysis. Figure 5 shows no discernible trends indicating a good model. Finally the regression equation was used to predict new values for the response variables with good accuracy validating the model selection.

# Fast, Physical, Predictive and Calibrated Modeling of Ion Implantation

## Introduction

Ion implantation has become a critical step for controlling ultra-shallow junctions, in sub-0.1mm CMOS technology. In a Research & Development environment, Technology Computer Aided Design (TCAD) is involved in the device optimization loop and requires efficient and predictive implantation modeling with frequent updating of the range of validity. For this purpose, semi-empirical models using statistical distributions are mainly chosen, because this kind of simulation is faster than the physically based Monte-Carlo (MC) approach. We propose a methodology which can be applied to ion implantation modeling with easy build-up, and which gives a predictive capability in the explored experimental domain. This calibration strategy will enhance the efficiency of analytical modeling by the combination the use of SIMS profile and the statistical qualities of Design of Experiments (DoE). Thus, only a few extra experiments are needed to extend the ion implantation simulation domain, in order to take into account the most advanced

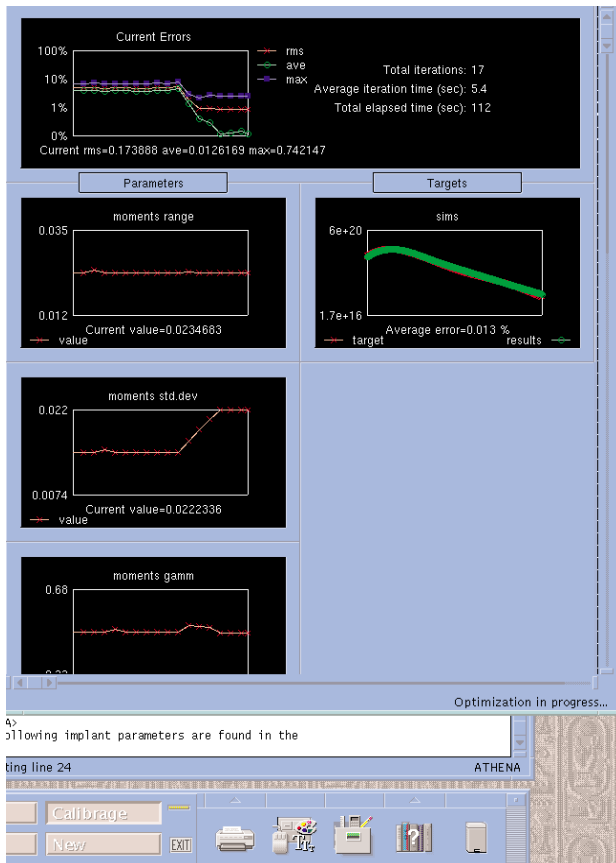


Figure 2: View of the *Optimizer* windows during extraction procedure.



Figure 1: Input deck used for Dual Pearson 4 moments extraction.

process conditions accurately. Our methodology is carried out for low energy B and As implantation, which is the case in practice for ultra-shallow junction engineering.

## Calibration of Ion implantation modeling

The results provided by a TCAD simulator are a function of both the experimental conditions and of the parameters of the used model, parameters which may themselves depend on the experimental conditions. In the case of analytic simulation of ion implantation, the tuning of the parameters (for example the moments of the statistical distribution) is often necessary, because they incorporate the experimental uncertainties. On the contrary, for MC computations, parameters are purely physical, so do not need to be adjusted.

The problem of predictive calibration of TCAD simulators has been previously addressed and an original methodology has been proposed [1]. The main idea is that a simulation can be considered as calibrated not only if the set of model parameters is fitted to particular experiments,

but also if the sensitivity of these parameters to the experimental process parameters, is determined. With this aim, the use of Design of Experiments (DoE) and Response Surface Modeling (RSM) permits the choice of the most significant experiments, to finally generate an empirical model for the parameters of the implantation model.

Nowadays, the parameters of the most advanced analytical ion implantation models, like the Dual-Pearson 4 (DP4) [2], are linearly interpolated in lookup tables to produce fast and accurate simulation.

However, these lookup tables suffer from several drawbacks:

- (i) default values in TCAD software must be calibrated and extended over the whole interesting range, to make the modeling results closer to the specific experimental conditions of each fab, in particular the dose loss;
- (ii) the global consistency of the table is not maintained when further parameter values are incorporated;
- (iii) a great number of experiments is required to obtain discrete sets of model parameters that cover the experimental domain with a sufficient accuracy.

The advantages of RSM could then fulfill the requirements of predictive calibration of ion implantation analytical models.

### Application to Advanced Analytical Models

We applied our strategy to the DP4 ion implantation modeling: we attempted to find a quadratic modeling of the parameters (Rp, DRp, skewness, kurtosis,...), of the DP4 models. To do that we have applied the following strategy:

- DoE on which SIMS profile will be extracted.

The domain of variation is shown on Table 1.

Factors	Energy	Dose As BF2 (at. cm <sup>-2</sup> )	Dose B (at. cm <sup>-2</sup> )	Tilt (deg)	Twist (deg)
range	3 to 10	3 10 <sup>13</sup> to 10 <sup>15</sup>	1 10 <sup>13</sup> to 5 10 <sup>14</sup>	7	27

Table 1: Experimental ranges for As, BF2 and B.

- Use of the SILVACO OPTIMIZER to extract moments of DP4 from experimental SIMS profile (Figure 1 and 2).
- Modelisation (RSM) of the DP4 moments. We found that the RSM of these models parameters, as function of the experimental process condition are satisfactory. Indeed the adjusted R<sub>c</sub> criterion value, which indicates the quality of the empirical models, is rarely below 0.8.

DP4 Bore	6.5					13.85				
	perte dose	range	sid	gamma	laurio	srange	ssid	sgamma	slaurio	dratio
constant	-39.76199676	0.023640226	0.021307672	0.263516364	6.451451973	0.031443518	0.05102664	-0.384083995	0	0.798281186
energy	4.60095233	0.00441488	0.002696733	0	0.360230967	0.00843254	0.004168205	-0.024255712	0	0.014443048
log_dose	-17.28823926	0	0	0.097169833	0	0.008265374	0	0	0	0.105622367
e*log_d	0	0	0	0	-0.589395063	0	0	0	0	0
energy <sup>2</sup>	3.68587733	-7.865E-05	0	0	0	0.000869942	-0.000612146	0	0	0.003917509
log_dose <sup>2</sup>	0	0.001265656	0	0.115668737	0	0	0	0	0	0

Figure 3. Coefficients of the analytical model for each SVDP model parameter as a function of the process parameters.

### Results

As already explained in [4], we have used the ability of **DeckBuild** to include any UNIX command inside any simulator input file. This feature authorizes users to include their own external routines inside **DeckBuild**. This is what we did in **ATHENA** to specify the values of the moments of the SIMS Verified Dual Pearson (SVDP) mode. The external routine contains the polynomial model that describes the SVDP model parameter (Rp for example) as a function of the process parameters like dose and energy (see Figure 3.). Figure 4 and 5 are an illustration of the profile obtained using this methodology for respectively Arsenic and Boron, SIMS profile was superimposed for comparison purpose.

In Figure 6, we show the global improvement over the whole As and B profile database, as compared to the

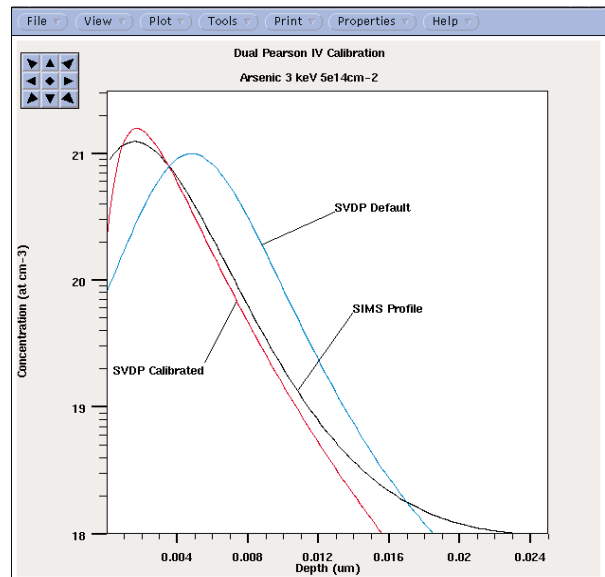


Figure 4: Arsenic profile in **TonyPlot** before and after calibration, comparison with SIMS profile.

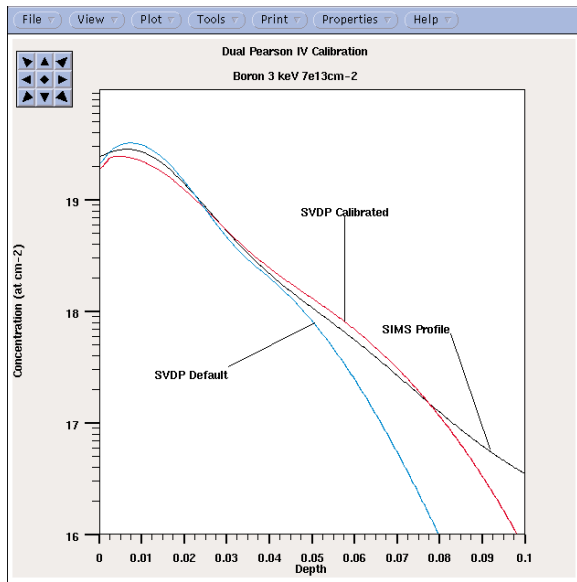


Figure 5: Boron profile in Tonyplot before and after calibration, comparison with SIMS profile.

simulations performed with the SVDP model of *ATHENA* [3]. The improvement is evaluated by the Root Mean Square Relative Error:

where  $y_{expi}$  and  $y_{simi}$  are respectively the  $i$ th experimental and simulated concentration values of a  $n$  points discretization of the profile.

### Influence on Device Characteristics

It is often recognized in the TCAD word that an accurate simulation of electrical MOSFET characteristics is primarily due to a good process simulation. This is illustrated as an example in the Figure 7 where we have made the same *ATLAS* simulation with two different *ATHENA* process simulation. One using the default value of the moments of the SVDP model and the other one using the calibrated one.

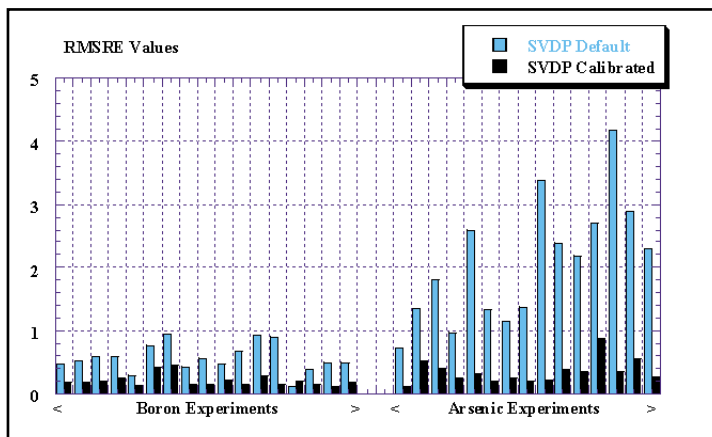


Figure 6: RMSRE for Arsenic and Boron which show the reduction after calibration, of the difference between SIMS profile and simulation.

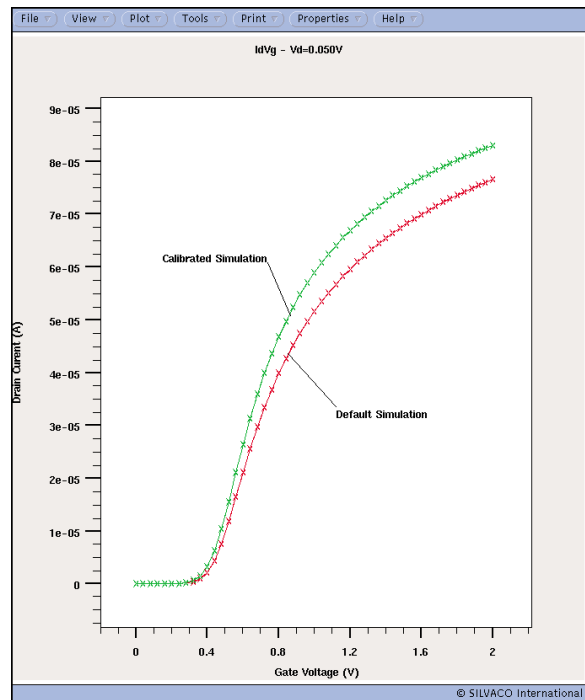


Figure 7: Comparison of the use of calibrated profiles on a device characteristic.

### Conclusion

In this study, we have presented an original and efficient methodology for global ion implantation modeling. The advantages of this methodology are a lower number of experiments, confidence in the values of the calibrated model parameters, and the rapid implementation of new data within our process simulator *ATHENA*. However it is of great importance to notice that the aim of this paper was to show a calibration methodology and not necessary to give new parameters for the SVDP implant model. Indeed it is not guaranty that replacing the default values by the values obtained from this work will give better results in all cases. The reason is that the confidence we have in the results done in this work could not be maintained if we take the values "out of their context". This is due to the high degree of dependency of the way of doing calibration (DoE used, optimizer setup..), making measurements and more important the Fab itself.

### References

- [1] G. Le Carval - SISPAD'97 - pp 177-180
- [2] A. F. Tash - J. Electrochem. Soc. 136(3) 1989 - pp 810-814
- [3] SILVACO International - *ATHENA User's Manual*
- [4] SILVACO *Simulation Standard* May 2000

# Calendar of Events

## August

1
2
3
4
5
6
7
8
9
10
11
12
13
14
15
16
17
18
19
20 2000 Topical on Hetro Structure Microelectronics – Kyoto, Japan
21 2000 Topical on Hetro Structure Microelectronics – Kyoto, Japan
22 2000 Topical on Hetro Structure Microelectronics – Kyoto, Japan
23 2000 Topical on Hetro Structure Microelectronics – Kyoto, Japan
24
25
26
27
28 Intl Conf on Solid State Devices and Materials, Sendai, Japan
29 Intl Conf on Solid State Devices and Materials, Sendai, Japan
30 Intl Conf on Solid State Devices and Materials, Sendai, Japan
31

## September

1
2
3 Japan Applied Physics - Hokkaido, Japan
4 Japan Applied Physics - Hokkaido, Japan
5 Japan Applied Physics - Hokkaido, Japan
6 Japan Applied Physics - Hokkaido, Japan SISPAD 2000-Seattle WA
7 Japan Applied Physics - Hokkaido, Japan SISPAD 2000-Seattle WA
8 SISPAD 2000-Seattle WA
9
10
11 ESSDERC, Cork, Ireland
12 ESSDERC, Cork, Ireland
13 ESSDERC, Cork, Ireland Int'l w/s on Power and Timing, Opt and Sim.-Germany
14 Int'l w/s on Power and Timing, Opt and Sim.-Germany
15 Int'l w/s on Power and Timing, Opt and Sim.-Germany
16
17
18
19
20
21
22
23
24
25 BCTM BiPOLAR- Minneapolis
26 BCTM BiPOLAR- Minneapolis
27 BCTM BiPOLAR- Minneapolis
28
29
30

## Bulletin Board



### III/V Compound Conference in Japan

Silvaco is heading to Japan August 20th through 23rd for the 2000 Hetero-Structure Microelectronics conference. Held this year in the Kyoto Research Park, our Japanese office will be introducing attendees to Silvaco products and answering questions about Silvaco's powerful suite of tools.



### Solid State Device and Materials Conference in Japan

August 28th through 31st Silvaco's Japanese office is headed to the Sendai International Center for the International Conference on Solid State Device and Materials. With benchmarks in reliability and speed, Silvaco tools enable developers to reduce the time spent on jobs and eliminate inefficiencies. Silvaco welcomes the opportunity



### Success Continues at Silvaco

As summer comes to a close Silvaco is ramping up for another busy fall stacked with exciting conferences worldwide. Life never slows at Silvaco, as development continues at breakneck speeds, and with the power to simulate the largest designs and the speed to keep users' design flows moving, Silvaco's pride lies in its customers' successes.

If you would like more information or to register for one of our workshops, please check our web site at <http://www.silvaco.com>

The Simulation Standard, circulation 18,000 Vol. 11, No. 8, August 2000 is copyrighted by Silvaco International. If you, or someone you know wants a subscription to this free publication, please call (408) 567-1000 (USA), (44) (1483) 401-800 (UK), (81)(45) 820-3000 (Japan), or your nearest Silvaco distributor.

Simulation Standard, TCAD Driven CAD, Virtual Wafer Fab, Analog Alliance, Legacy, ATHENA, ATLAS, MERCURY, VICTORY, VYPER, ANALOG EXPRESS, RESILIENCE, DISCOVERY, CELEBRITY, Manufacturing Tools, Automation Tools, Interactive Tools, TonyPlot, TonyPlot3D, DeckBuild, DevEdit, DevEdit3D, Interpreter, ATHENA Interpreter, ATLAS Interpreter, Circuit Optimizer, MaskViews, PSTATS, SSuprem3, SSuprem4, Elite, Optolith, Flash, Silicides, MC Depo/Etch, MC Implant, S-Pisces, Blaze/Blaze3D, Device3D, TFT2D/3D, Ferro, SiGe, SiC, Laser, VCSELS, Quantum2D/3D, Luminous2D/3D, Giga2D/3D, MixedMode2D/3D, FastBlaze, FastLargeSignal, FastMixedMode, FastGiga, FastNoise, Mocasim, Spirt, Beacon, Frontier, Clarity, Zenith, Vision, Radiant, TwinSim, , UTMOST, UTMOST II, UTMOST III, UTMOST IV, PROMOST, SPAYN, UTMOST IV Measure, UTMOST IV Fit, UTMOST IV Spice Modeling, SmartStats, SDDL, SmartSpice, FastSpice, Twister, Blast, MixSim, SmartLib, TestChip, Promost-Rel, RelStats, RelLib, Harm, Ranger, Ranger3D Nomad, QUEST, EXACT, CLEVER, STELLAR, HIPEX-net, HIPEX-r, HIPEX-c, HIPEX-rc, HIPEX-crc, EM, Power, IR, SI, Timing, SN, Clock, Scholar, Expert, Savage, Scout, Dragon, Maverick, Guardian, Envoy, LISA, ExpertViews and SFLM are trademarks of Silvaco International.

# Hints, Tips and Solutions

William French, Applications and Support Manager

## Q. Can ATLAS be used to simulate advanced III-V or II-VI materials ?

A. Yes. **ATLAS** now supports a wide range of materials in its database. This database covers single element conductors, binary compounds and quaternary compounds. A complete list of all materials can be found in Appendix B of the *ATLAS Users Manual Vol. II*.

It should be noted however, that many of these materials are quite recent and do not have a comprehensive set of physical parameters or physical models yet available. Atlas can still be used to simulate these devices but requires three contributions from the user.

First, the user should ensure that a complete set of physical parameters are available. To illustrate this the material InAlAs will be invoked within an input deck. To check the required physical parameters are available before a simulation is started the following command should be written within the input deck

### MODEL PRINT

This will then produce in the runtime output window of deckbuild the following table when two regions are present, GaAs and InAlAs :

#### REGIONAL MATERIAL PARAMETERS:

```
Region : 1 2
Material : GaAs InAlAs
Type : semicond. semicond.
Epsilon : 13.2 0
```

#### BAND PARAMETERS

```
Eg (eV) : 1.42 2.1
Chi (eV) : 4.07 0
Nc (per cc) : 4.35e+17 1
Nv (per cc) : 8.16e+18 1
ni (per cc) : 2.12e+06 2.29e-18
Gc : 2 2
Gv : 4 4
Ed (eV) : 0.044 0.044
Ea (eV) : 0.045 0.045
```

#### RECOMBINATION PARAMETERS

```
Lifetime (el): 1e-09 1
Lifetime (ho): 2e-08 1
Auger cn : 5e-30 0
Auger cp : 1e-31 0
Auger kn : 0 0
Auger kp : 0 0
Copt : 1.5e-10 0
An** : 6.29 110
Ap** : 105 30
```

#### IMPACT IONIZATION MODEL PARAMETERS (SELBERHERR MODEL)

```
betan : 1.82 1
betap : 1.75 1
egran : 0 0
an1 : 1.9e+05 8.6e+06
bn1 : 5.75e+05 3.5e+06
an2 : 1.9e+05 8.6e+06
an2 : 5.75e+05 3.5e+06
ap1 : 2.22e+05 2.3e+07
bp1 : 6.57e+05 4.5e+06
ap2 : 2.22e+05 2.3e+07
bp2 : 6.57e+05 4.5e+06
```

#### SATURATION VELOCITIES

```
Vsatsn (cm/s) : 7.7e+06 1e+06 1e+06
Vsatp (cm/s) : 7.7e+06 1e+06 1e+06
```

As shown, the material InAlAs does not have certain parameters predefined such as epsilon and Chi. The user is required to define these parameters, all the Band Parameters and any Recombination and Impact Ionization Parameters required in the model definitions. In this case the necessary **ATLAS** statement could be:

```
material material=InAlAs permittivity=13.9
nc300=1.5e17 nv300=8.1e18 affinity=3.6 eg300=1.47
taun0=1.2e-9 taup0=1.2e-9
```

Second, the physical parameters inbuilt into **ATLAS/Blaze** cover GaAs, AlGaAs, InGaASP, SiGe and SiC. For advanced materials either constants values need to be used or the C-interpretter is required. For instance, the bandgap in these materials is a function of either the x or y or both mole fractions. If a graded mole fractions is required in a device the user has to use the C-interpretter to define the variation of bandgap with the x or y mole fraction.

Third, there are a limited set of physical models available within **ATLAS/Blaze**, such as for mobility. The C-interpretter should therefore be applied by the user to define relevant and accurate physical models for the material they are studying.

### Call for Questions

If you have hints, tips, solutions or questions to contribute, please contact our Applications and Support Department  
Phone: (408) 567-1000 Fax: (408) 496-6080  
e-mail: [support@silvaco.com](mailto:support@silvaco.com)

### Hints, Tips and Solutions Archive

Check our our Web Page to see more details of this example plus an archive of previous Hints, Tips, and Solutions  
[www.silvaco.com](http://www.silvaco.com)

# Your Investment in Silvaco is SOLID as a Rock!!

While others faltered, Silvaco stood SOLID for 15 years. Silvaco is NOT for sale and will remain fiercely independent. Don't lose sleep, as your investment and partnership with Silvaco will only grow.

## **SILVACO** INTERNATIONAL

### **USA HEADQUARTERS**

**Silvaco International  
4701 Patrick Henry Drive  
Building 2  
Santa Clara, CA 95054  
USA**

**Phone: 408-567-1000  
Fax: 408-496-6080**

**sales@silvaco.com  
www.silvaco.com**

### **CONTACTS:**

**Silvaco Japan**  
jpsales@silvaco.com

**Silvaco Korea**  
krsales@silvaco.com

**Silvaco Taiwan**  
twsales@silvaco.com

**Silvaco Singapore**  
sgsales@silvaco.com

**Silvaco UK**  
uksales@silvaco.com

**Silvaco France**  
frsales@silvaco.com

**Silvaco Germany**  
desales@silvaco.com

*Products Licensed through Silvaco or e\*ECAD*

